RAPID COMMUNICATIONS

PHYSICAL REVIEW B VOLUME 51, NUMBER 7 15 FEBRUARY 1995-I

Dislocations and the reconstruction of (111) fcc metal surfaces

C. B. Carter* and R. Q. Hwang
Advanced Materials Research Department, Sandia National Laboratories, Livermore, California 94550
(Received 17 October 1994)

It is shown that a pair of hexagonal dislocation structures can be used as a basis for understanding the herringbone pattern and the node networks that have been observed in the structure of several (111) metal surfaces and overlayers. The hexagons are composed of the dissociation patterns of perfect edge dislocations, which are derived from the well-known concepts of the Thompson tetrahedron. At each corner there is a unit threading dislocation; the actual location of this dislocation alternates between the inner and outer Shockley partial dislocation. One of the hexagons will form when there is an excess of vacancies in the surface layer, the other when there are excess atoms. The hexagons can each be reduced to give a corresponding threefold node also terminated by threading dislocations. From such a model, structural characteristics of (111) surface reconstructions such as the presence of perfect edge dislocations on only one side of the stacking fault, can be understood. Whether the herringbone pattern or the node array will be observed in a particular case will depend on the details of the specific systems. In particular, the balance between the mechanisms of the dislocation pattern formation and the equilibrium configuration may be important. The threading dislocations play a critical role in these processes.

The (111) surfaces of several pure metals and metallic overlayers have been observed to exhibit strain-induced surface structures. These structures result from the density differences between the surface layer and the underlying substrate. An interesting characteristic of the patterns is that they can be categorized into two general types of patterns: (a) a striped pattern that, following previous work, we will refer to as the herringbone[1] and (b) triangular networks. Examples of these two categories can be found in a number of systems such as the extensively studied Au(111) surface reconstruction, the Pt(111) surface reconstruction, and several thin-film systems. We will refer to the Au(111) and Pt(111), respectively, as examples of these two types of patterns. In this paper we propose a hexagonal model of (111) surface dislocations that provides a basis for the understanding of both types of structures. In particular, it will demonstrate the importance of surface threading dislocations to the formation of these patterns.

The most extensively studied of these systems is that of the herringbone structure of Au(111). The surface-layer density difference, to our knowledge, was first observed by transmission-electron-microscopy (TEM) measurements.[2,3] Later diffraction studies[4,5] identified the TEM features as being due to a $p\times 1$ reconstruction, where $p=23\pm 1$ (also known as the $23\times\sqrt{3}$ structure).[6–9] This results from a surface-layer contraction of approximately 4%. Along the close-packed $\langle 1\bar{1}0\rangle$ direction, 23 surface atoms are matched with 22 substrate (second layer) atoms. In the orthogonal $\langle 11\bar{2}\rangle$ direction, the surface spacing is in close registry with the bulk. This results in the formation of domains of the $p\times 1$ structure, which can occur in each of three allowed directions on the threefold-symmetric (111) surface. The domains link to form the herringbone pattern as shown schematically in Fig. 1(a). In this figure the pairs of bold lines represent Shockley partial dislocations,[10] which have their cores located between the surface layer and the second layer in the bulk material. The second and subsequent layers are not reconstructed although TEM observations[7–9] show that the strain fields of these dislocations do extend into the bulk, i.e., the surface layer does in fact influence the bulk (substrate) crystal.

The straight segments of these partial dislocations are both in 60° orientations, with respect to their Burgers vectors, and are separated by a stacking fault that corresponds to atoms of the surface layer located at hcp sites. The nomenclature used throughout this paper to identify the regions of misfit will be that of dislocation theory and the Burgers vectors will be denoted with reference to Thompson's tetrahedron[11] as summarized by Hirth and Lothe.[12] These Shockley partial dislocations have been referred to elsewhere as solitons[13] and domain walls separating differently oriented elastic stresses.[14] The domain-wall terminology comes from the fact that the partial dislocations separate regions of fcc and hcp stacking of the surface layer.

These dislocations accommodate the misfit between the surface layer and the bulk so they are also referred to as misfit dislocations, a term that we will use. The straight lengths consist of two 60° Shockley partial dislocations giving a total dislocation of edge character. Such a perfect dislocation is then in the most efficient orientation to accommodate misfit.

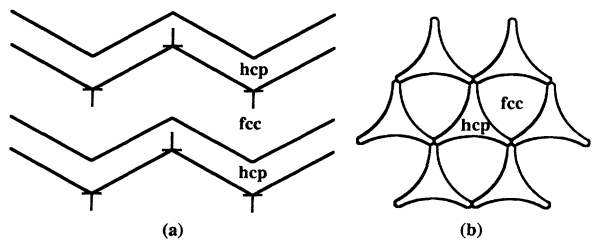

FIG. 1. Schematics of the reconstructed (111) surface of Au. (a) The herringbone structure; (b) the appearance of a node network.

A critical contribution to the understanding of this surface structure was provided by scanning tunneling microscopy (STM) through the demonstration that end-on perfect dislocations are present at the bends in the herringbone pattern.[15,16] Furthermore, these dislocations, which are recognized by the terminating surface lattice planes in the STM image, not only reverse their sign at alternating bends, but are always associated with only one side of the stacking-fault ribbon as indicated in Fig. 1. Since these dislocations run from the interface to the surface, we will refer to them as threading dislocations to conform to the standard terminology of epitactic growth. It is clear that these threading dislocations are a necessary complement to the herringbone arrangement of misfit dislocations.

One reason that these end-on dislocations are important is that they have been shown directly to influence the growth of subsequent material.[17–19] For example, it has been shown[17] that at $\frac{1}{10}$-ML coverage of Ni on Au(111), every dislocation site was already decorated by a Ni island. It will also be shown in a subsequent extended paper that these end-on dislocations directly influence the further rearrangement of the surface layer.

While the geometry described above is found for the reconstructed Au(111) surface and for heteroepitaxial systems,[20,21] it has been found that when Pt is grown on the Pt(111) surface[22,23] threefold star-shaped features appear. These "stars" can eventually link together to form a hexagonal network of dislocations as illustrated in Fig. 1(b). The question arises as to whether these two structures are related. Evidence suggesting that they are has been provided by a study of the effect of depositing partial layers of alkali metals on reconstructed Au(111) surfaces;[23] the effect is a transformation from the herringbone pattern to a node network.

Our model of these reconstruction patterns is based on the two nonequivalent hexagonal dislocation loops shown in Fig. 2 together with a Thompson tetrahedron. The tetrahedron is labeled ABC clockwise and D is directly below δ, the midpoint of the triangle. (Unfortunately the corners of the Thompson tetrahedron are always labeled $ABCD$ and this has no relation to the $ABCABC$ notation used to denote the fcc stacking sequence; this sequence will be $QRSQRS$ in the notation given in Fig. 2.) From an atomistic viewpoint this corresponds to the second layer having atoms at the R sites and the reconstructed fcc first layer having atoms at the S sites. If the first-layer atom is moved to an S site, it will be in the hcp position relative to the bulk material.

The Thompson tetrahedron rotating gives us a simple way to remember the order and sign of the partial dislocations present along dissociated dislocations. The rule is that if we look at the dislocation on its glide plane from outside the tetrahedron as in Fig. 2, then the greek letter must be placed outside the stacking-fault ribbon for the stacking fault to be a simple intrinsic stacking fault as required here, i.e., a surface layer located in the hcp site relative to the second and third layers. Thus the dislocation with Burgers vector AB in Fig. 2(a) is composed of two partial dislocations $A\,\delta$ and δB with δB appearing on the left side and $A\,\delta$ on the right. The two hexagons have been labeled accordingly. The reader is referred to Ref. 12 for a detailed discussion of the Thompson tetrahedron.

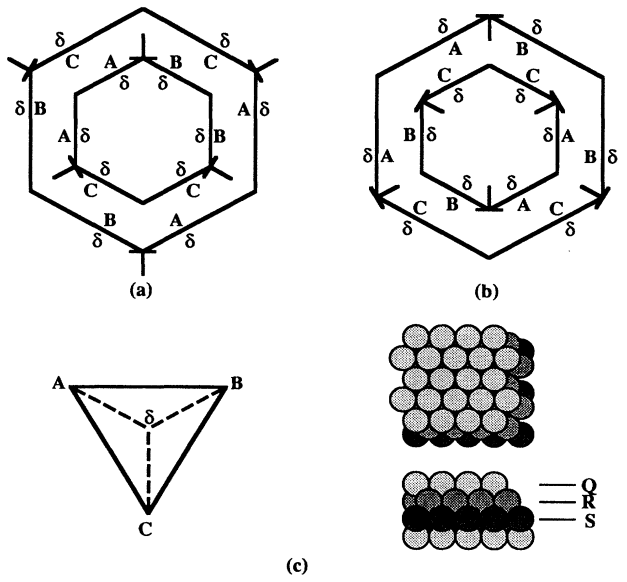

FIG. 2. A pair of hexagons summarizing the location and Burgers vectors of both the misfit Shockley partial dislocations and the threading dislocations. The Thompson tetrahedron is shown in (c) together with a schematic showing the three positions that can be occupied by close-packing atoms. The sequence $QRSQRS$ here corresponds to fcc stacking.

Threading dislocations are present in Fig. 2 wherever the label on the Shockley partial dislocation changes. For example, when δB and δC meet (Burgers vectors δB and $C\,\delta$ when both are viewed looking into the node), a threading dislocation with Burgers vector CB (looking out of the node) is formed. In either case there are three threading dislocations on the inner partial-dislocation hexagon and three on the outer one.

It is important to remember that the finish to start right-handed/perfect-crystal convention for the Burgers circuit is implicit throughout this discussion.[12] When the dislocation is viewed along its line direction with its glide plane being horizontal, the extra half plane is above the plane if the Burgers vector points to the left and below the glide plane if its points to the right. The important difference between the two hexagons is that in one case all the extra half planes (denotes by the upright in the T) point towards the center of the hexagon, while in the other case they all point away from the center. This difference is crucial. The Shockley partial dislocations can glide on the (111) plane, a feature that will be important in interpreting the threefold star configuration. However, the threading dislocations cannot; their glide planes are determined by their Burgers vectors since they have unit length.[24] For example, any two of the three threading dislocations could, in principle, coalesce by glide but they can never meet the third threading dislocation by glide alone. Furthermore, the hexagonal loops cannot form by glide alone even though the dislocations in the (111) plane are all Shockley partial dislocations.

This implies that in order for the loops to expand the threading dislocations must climb by absorbing vacancies [Fig. 2(a)] or interstitial atoms [Fig. 2(b)]; i.e., each pair of

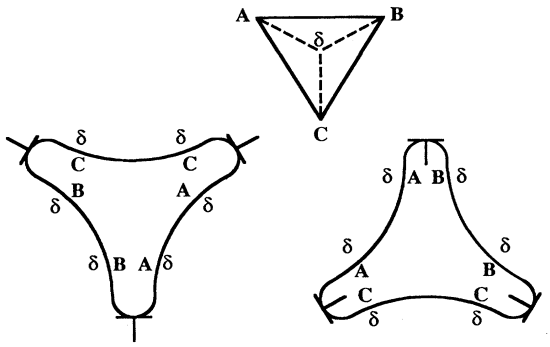

FIG. 3. A pair of threefold star nodes derived from the hexagons in Fig. 2 by removing the inner hexagon and allowing the outer one to relax.

two hexagons (inner and outer) could only have expanded to the size shown in Fig. 2 by the appropriate mechanism of absorbing point defects. Thus the hexagon shown in Fig. 2(a) can only form and grow if the surface layer contains an excess of vacancies. Similarly the hexagon shown in Fig. 2(b) can only form and grow if the surface layer contains excess atoms, which is precisely the situation that occurs in the Au(111) and Pt(111) surfaces.

Although the pairs of configurations in Figs. 2 and 3 appear to be very similar, they cannot be related to one another by a simple 180° rotation about the [111] axis because the (111) surface only has a threefold rotation axis, as can be readily appreciated by considering the tetrahedron in Fig. 2(c). Only one orientation of the defect will appear in a particular surface.

We can construct a related pair of dislocation configurations as shown in Fig. 3 by removing the inside hexagons in Fig. 2. If we keep the outer threading dislocations fixed in place (i.e., not changing the number of excess point defects associated with their outer hexagon), the convex Shockley partial dislocations will become concave moving inwards to minimize the total surface energy associated with the hcp (surface stacking fault) region but the apexes will be unchanged. The resulting three-pointed star corresponds to the defect reported in Pt films grown on Pt(111) and Cu grown on Ru(0001).[22,25–27]

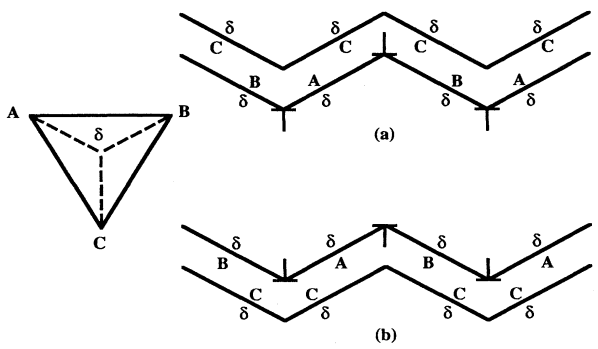

FIG. 4. A pair of herringbone segments, one constructed from the hexagon in Fig. 2(a) and the other from that in Fig. 2(b).

An interesting feature of these star configurations is that, as borne out by the experimental observations, the Shockley partial dislocations each curve through the edge orientation while changing from one 60° orientation to the other. This observation implies that the misfit Shockley partial dislocation have a line energy (line tension) analogous to the corresponding line defect in the bulk crystal although, of course, the actual magnitude of this energy is expected to be different. The defects shown in Fig. 3 correspond to extended P nodes in the terminology of Frank (as defined in Ref. 12). If the threading dislocations at the tops of three such nodes come together, a threefold node can be formed that does not contain any threading dislocations. This defect is referred to as the K node and corresponds to the "bright star" reported by Bonn *et al.*[22]

We are now able to understand the details of the herringbone pattern shown in Fig. 1(a). Looking as the inclined segments of the hexagons in Fig. 2 we notice that the two dislocations AC and CB are present on both the top and bottom sloping segments. We can therefore form herringbone chains by alternating these segments as shown in Fig. 4. In fact, all three orientations of the herringbone can be created by using opposing dislocation segments of the hexagon. From this construction it is again clear that we cannot mix segments from Fig. 2(a) with segments from Fig. 2(b) since the order of the partial dislocations does not match. The result is that the threading dislocation always appear on only one side of the stacking fault as is experimentally observed. Again the configuration in Fig. 4(a) cannot be rotated to give that in Fig. 4(b).

The configurations in Fig. 4 can only arise under the same circumstances as could lead to the presence of the corresponding hexagon, i.e., Fig. 4(a) results from an excess of surface vacancies while 4(b) is created by an excess of surface atoms. This conclusion can be confirmed by the gedanken experiments of increasing the amplitude (A) of the herringbone pattern from zero to that shown in Fig. 4(b) while keeping the wavelength ($2L$) constant. The threading dislocations along the misfit dislocation can only move to the configuration shown in Fig. 4(b) by absorbing interstitial atoms, i.e., extra atoms present in the Au(111) surface.

The existence of the threading dislocations is crucial to the overall strain-relief mechanisms in these systems. The extra half planes of atoms or vacancies allow the misfit to be accommodated in a more symmetric mode. The details of the role of the dislocations in this misfit accommodation is beyond the scope of this paper and will be addressed in a forthcoming paper.

The arrays of threading dislocations also influence the surface structure in a more subtle way. Each array is a tilt grain boundary with the angle of tilt being opposite for neighboring arrays. The effect of a tilt boundary is to rotate the grains on either side relative to one another. Since the threading dislocations are only present in the surface layer, this means that the surface layer is rotated relative to the second layer (i.e., the bulk crystal). These tilt boundaries are usually symmetric although exceptions have been reported (e.g., Ref. 28). The distance between dislocations in the arrays is typically 73 Å (Ref. 15) and the Burgers vector of the

$\frac{1}{2}\langle 110\rangle$ threading dislocation is defined with respect to the surface monolayer (2.77 Å).[15] The usual relationship

$$\sin\theta/2 = b/2D$$

gives a rotation on each side of the boundary of 0.45°, i.e., the arrays are 0.9° tilt boundaries. This means that the $\langle 112\rangle$ and $\langle 110\rangle$ rows of atoms are sheared through an angle of 0.45° relative to the underlying crystal. Over the length between threading-dislocation boundaries the atoms are actually displaced laterally by ~1.4 Å (taking $L/\cos 30°$ to be 173 Å), which can be compared with an experimentally determined value of 0.9 Å.[16]

In summary, the model represented by the pair of hexagons shown in Fig. 2 can be used as a basis for understanding the herringbone pattern and the node networks seen in the reconstruction of several (111) metal surfaces. In a subsequent paper we will discuss the implications of this model more fully. For example, the threading dislocations can be thought of as unit jogs that will dissociate to some extent (perhaps three or so atomic distances). Thus threading partial dislocations with a screw component cause a small step on the (111) surface and provides a preferred structural site for the growth of second-layer nuclei as occurs in Ni deposited on Au. Clearly the threading dislocations play a critical role in this process.

The authors acknowledge valuable discussions with Dr. J. L. Stevens, Dr. J. C. Hamilton, Dr. S. M. Foiles, and Dr. D. D. Chambliss, and the encouragement of Dr. W. G. Wolfer and Dr. M. I. Baskes. This work was supported by the Office of Basic Energy Science, Division of Materials Science, of the U.S. Department of Energy under Contract No. DE-AC04-94AL85000.

*Permanent address: Department of Chemical Engineering and Materials Science, Amundson Hall, U. of Minnesota, 421 Washington Ave., SE, Minneapolis, MN 55455.

[1] R. J. Wilson, S. Chiang, and D. D. Chambliss, Aust. J. Phys. **43**, 393 (1990).
[2] T. P. Darby and C. M. Wayman, Philos. Mag. **30**, 1171 (1974).
[3] K. Yagi *et al.*, Surf. Sci. **86**, 174 (1979).
[4] J. Perdereau, J. P. Biberian, and G. E. Rhead, J. Phys. F **4**, 798 (1974).
[5] H. Melle and E. Menzel, Z. Naturforsch. Teil A **33**, 282 (1978).
[6] J. C. Heyraud and J. J. Metois, Surf. Sci. **100**, 519 (1980).
[7] Y. Tanishiro, H. Kanamori, K. Takayanagi, K. Yagi, and G. Honjo, Surf. Sci. **111**, 385 (1981).
[8] K. Yagi, K. Kobayashi, Y. Tanishiro, and K. Takayanagi, Thin Solid Films **126**, 95 (1985).
[9] K. Takayanagi, Y. Tanishiro, K. Yagi, K. Kobayashi, and G. Honjo, Surf. Sci. **205**, 637 (1988).
[10] C. Wöll, S. Chiang, R. J. Wilson, and P. H. Lippel, Phys. Rev. B **39**, 7988 (1989).
[11] N. Thompson, Proc. Phys. Soc. London Sect. B **66**, 481 (1953).
[12] J. P. Hirth and J. Lothe, *Theory of Dislocations* (Krieger, Malabar, FL, 1992).
[13] Y. Okwamoto and K. H. Bennemann, Surf. Sci. **186**, 511 (1987).
[14] O. L. Alerhand, D. Vanderbilt, R. D. Meade, and J. D. Joannopoulos, Phys. Rev. Lett. **61**, 1973 (1988).
[15] D. D. Chambliss, R. J. Wilson, and S. Chiang, J. Vac. Sci. Technol. B **9**, 933 (1991).
[16] J. V. Barth, H. Brune, G. Ertl, and R. J. Behm, Phys. Rev. B **42**, 9307 (1990).
[17] D. D. Chambliss, R. J. Wilson, and S. Chiang, Phys. Rev. Lett. **66**, 1721 (1991).
[18] J. A. Stroscio, D. T. Pierce, R. A. Dragoset, and P. N. First, J. Vac. Sci. Technol. A **10**, 1981 (1992).
[19] J. Wollschläger and N. M. Amer, Surf. Sci. **277**, 1 (1992).
[20] H. Brune, H. Röder, C. Boragno, and K. Kern, Phys. Rev. B **49**, 2997 (1994).
[21] G. O. Pötschke and R. J. Behm, Phys. Rev. B **44**, 1442 (1991).
[22] M. Bott, M. Hohage, T. Michely, and G. Comsa, Phys. Rev. Lett. **70**, 1489 (1993).
[23] J. V. Barth, R. J. Behm, and G. Ertl, Surf. Sci. Lett. **302**, L319 (1994).
[24] L. Bragg and J. F. Nye, Proc. R. Soc. London Ser. A **190**, 474 (1947).
[25] Y. Hasegawa and P. Avouris, Science **258**, 1763 (1992).
[26] Y. Hasegawa and P. Avouris, J. Vac. Sci. Technol. B **12**, 1797 (1994).
[27] C. Günther, J. Vrijmoeth, R. Q. Hwang, and R. J. Behm, Phys. Rev. Lett. (to be published).
[28] E. I. Altman and R. J. Colton, J. Vac. Sci. Technol. B **12**, 1906 (1994).